

N O T I C E

THIS DOCUMENT HAS BEEN REPRODUCED FROM
MICROFICHE. ALTHOUGH IT IS RECOGNIZED THAT
CERTAIN PORTIONS ARE ILLEGIBLE, IT IS BEING RELEASED
IN THE INTEREST OF MAKING AVAILABLE AS MUCH
INFORMATION AS POSSIBLE



Technical Memorandum 80576

On the Angular Variation of Solar Reflectance of Snow

B. J. Choudhury and A. T. C. Chang

(NASA-TM-80576) ON THE ANGULAR VARIATION OF
SOLAR REFLECTANCE OF SNOW (NASA) 26 p
HC A03/MF A01 CSCL 08L

N80-12536

G3/43 Unclass
41479

OCTOBER 1979

National Aeronautics and
Space Administration

Goddard Space Flight Center
Greenbelt, Maryland 20771

TM 80576

ON THE ANGULAR VARIATION OF SOLAR REFLECTANCE OF SNOW

B. J. Choudhury
Computer Sciences Corporation
Silver Spring, Maryland 20910

and

A. T. C. Chang
Laboratory for Atmospheric Science (GLAS)
Goddard Space Flight Center
Greenbelt, Maryland 20771

October 1979

GODDARD SPACE FLIGHT CENTER
Greenbelt, Maryland 20771

Page intentionally left blank

CONTENTS

| | <u>Page</u> |
|---|-------------|
| Abstract | v |
| I. Introduction | 1 |
| II. Formulation of the Reflectance | 3 |
| III. Illustrative Numerical Results | 11 |
| IV. Conclusions | 19 |
| References | 20 |

LIST OF TABLES

| <u>Table</u> | | <u>Page</u> |
|--------------|---------------------------------------|-------------|
| 1 | Directional Surface Reflectance | 11 |

LIST OF ILLUSTRATIONS

| <u>Figure</u> | | <u>Page</u> |
|---------------|--|-------------|
| 1 | Spectral Variation of Incident Solar Flux | 15 |
| 2 | Spectral Reflectance of Snow for Different Grain Size for Solar Elevation of 30° | 16 |
| 3 | Spectral Reflectance of Snow for Different Solar Elevations (Grain Radius = 0.1 mm) | 17 |
| 4 | Dependence of Snowcover Albedo on Solar Elevation | 18 |

Page intentionally left blank

ON THE ANGULAR VARIATION OF SOLAR REFLECTANCE OF SNOW

B. J. Choudhury
and
A. T. C. Chang

ABSTRACT

Spectral and integrated solar reflectance of non-homogeneous snowpacks are derived assuming surface reflection of direct radiation and subsurface multiple scattering. For surface reflection, a bidirectional reflectance distribution function derived for an isotropic Gaussian faceted surface is considered, and for subsurface multiple scattering, an approximate solution of the radiative transfer equation is studied. Solar radiation incident on the snowpack is decomposed into direct and atmospherically scattered radiation. Spectral attenuation coefficients of ozone, carbon dioxide, water vapor, aerosol and molecular scattering are included in the calculation of incident solar radiation. Illustrative numerical results are given for a case of North American winter atmospheric condition. The calculated dependence of spectrally integrated directional reflectance (or albedo) on solar elevation is in qualitative agreement with available observations.

I. Introduction

Fast growth in world population imposes higher demands on available water supplies. To meet this increased demand, existing water supplies will have to be managed more effectively. Runoff from melting snow provides greater than 65% of the total streamflow across most of the mountainous Western United States. In the upper midwest of United States and the Canadian high plains, knowledge of snowpack characteristics is extremely valuable for flood forecasting purposes in the early spring. In addition, snowpacks also play an important role in climatic changes (References 1, 2, 3 and 4).

The variations of solar radiation absorbed and reflected by the Earth are key factors in the understanding of climatic change. In a simple energy feedback mechanism of climatic change, if solar radiation reflected by the Earth were increased, a trend towards the extension of the winter season will result (Budyko-Kukla type mechanism of ice cap, Reference 5). In this context, the role of snowpack need not be overemphasized because it is one of the most reflective naturally occurring materials. An understanding of visible near-infrared solar reflectance of snow is needed for mapping of snowcovered areas via remote sensing methods, and estimating the solar energy reflected by the Earth.

The complicated processes of reflectivity by a medium such as water, sand, vegetation or snow depend upon surface and subsurface radiative scattering and absorption characteristics. In general, the reflected radiation can be decomposed into two components: (1) specular and (2) diffuse. Radiation reflected in accordance with geometrical optics is the specular component, while radiation reflected according to the Lambertian law is the diffuse component. The relative contribution of these components varies with the physical characteristics of the medium and the zenith angles of radiation source and observation. Quantitative calculation of these two components will provide important information toward the understanding of the reflective process of solar radiation.

Snowpack is a complex and highly variable dielectric medium (References 6 and 7). It is continuously undergoing metamorphism due primarily to interaction with the atmosphere. Direct deposition of water vapor on the snow surface will lead to the formation of large (about 0.5 cm) faceted grains called surface hoar. Under constant below-freezing temperatures, the grains are generally well-rounded and their sizes vary from a fraction of a millimeter to about one millimeter. The effect of a temperature gradient will produce oblong and faceted grains whose sizes vary from about a millimeter to a few millimeters. The melt-freeze process leads to irregular globular masses of polycrystalline grains and the formation of surface crust. A model of snow will be a medium of randomly placed ice grains suspended in air and connected by intergranular bonds.

The "snow surface" is very different from the surface of other media (Reference 8). It could be considered as the diffuse interface between two media with different refractive indices. Large scale surface roughness may develop due to wind action. Ripples and wavelike structures are commonly observed in prairie snowpacks. Surface slope variation will cause nonuniform solar heating and consequently nonuniform metamorphism. Local melting and fusion are expected to cause horizontal inhomogeneity. The commonly observed glittering of snow on sunny days is vivid evidence of the mirror-like reflection by microareas of the surface.

The reflectance of snow shows a strong spectral dependence; moreover, it changes with solar elevation and cloudiness (References 9 and 10). The reflectance is high (0.9) for visible radiation and low (0.3) for near-infrared radiation. Although the shape of the reflectance curve does not change with the advancing of snow metamorphism, the magnitude for different portions of the curve does vary. At high solar elevations snow reflects as a diffuse reflector, but at low elevations it showed specular characteristics (Reference 9). For a completely overcast condition, snow surface behaves like a diffuse reflector (References 10 and 11).

Recent developments in remote sensing via visible and near-infrared radiometers provide great opportunity to gather information over snow covered areas. In fact, a data base of snow observations

collected by different satellites already exists. These observations have been made at different solar zenith angles and view angles as well as different spectral ranges. Understanding the basic reflective properties of snow is needed in order to analyze both the currently available and forthcoming observations. These analyses indicate the calculation of hemispheric reflectance (i.e., radiation reflected in all directions) from a limited number of angular observations and calculations of the total solar energy reflected from a limited number of spectral band observations (Reference 9, 12, 13 and 14).

The theoretical understanding of solar reflectance of snow should be based upon a model which can explain the various aspects of its spectral and angular reflection characteristics. In this respect, the existing models are not completely satisfactory. Existing models can be classified into two categories. One set of models attempts to explain the spectral reflection characteristics, while the other set explains the angular variations (References 8, 10, 15 and 16). A formulation therefore is needed to provide a unified description of both the spectral and angular variations of reflectance. This paper attempts to provide a unified theory for the reflection characteristics of snowpack. Numerical results derived from the model are presented and compared with observations.

II. Formulation of the Reflectance

The reflective processes of a dielectric medium depend upon surface and subsurface scattering and absorption characteristics. The theory of the angular variation of reflected radiation developed in Reference 8 is based on the theories developed to explain the reflection characteristics of unpolished dielectric surfaces (see also Reference 17). The surface is modeled as a collection of randomly oriented facets, each of which reflects like a small mirror. The angular distribution of the incident collimated radiation, as reflected by this collection of facets, depends directly on how the mirrors are oriented with respect to the mean smooth surface. The understanding of spectral reflectance is based upon surface and subsurface multiple scattering by ice grains (References 15 and 16).

Scattering and absorption by ice grains depend upon their size and shape as well as the refractive index of ice. Due to spectral variation of the refractive index, the scattering and absorption coefficients (and hence the reflectance itself) vary with wavelength. Application of the radiative transfer theory to this multiple scattering problem led to a spectral reflectance which agreed well with observations (Reference 16). These two different processes will be discussed in the following sections.

(1) Surface Reflection

The intensity of solar radiation on the snow surface can be written as:

$$I_1(\theta, \phi) = \frac{F_0}{\mu} g \delta(\mu - \mu_0) \delta(\phi) + (1 - g) \frac{F_0}{\pi} \quad (2-1)$$

where

F_0 = total spectral flux incident on the snow surface

g = ratio of direct and total spectral fluxes incident on the surface

$\mu_0 = \cos \theta_0$

$\mu = \cos \theta$

ϕ = azimuth angle of direct radiation.

The first term on the right side of Equation (2-1) is the direct radiation and the second term is the diffuse radiation. Subscripts for wavelength dependence will be omitted to simplify the notation.

At the snow surface, part of the direct radiation will be reflected back into the atmosphere. If $f_r(\theta, \phi; \theta', \phi')$ denotes the bidirectional reflectance distribution function of the surface, then the intensity I_r and the flux F_r of the reflected radiation may be obtained from the following equations:

$$I_r(\theta', \phi') = \int_0^{2\pi} d\phi \int_0^1 d\mu \mu f_r(\theta, \phi; \theta', \phi') I_d(\theta, \phi) \quad (2-2)$$

$$F_r = \int_0^{2\pi} d\phi' \int_0^1 d\mu' \mu' I_r(\theta', \phi') \quad (2-3)$$

where

$$\mu' = \cos \theta'$$

$$I_d(\theta, \phi) = \frac{F_0}{\mu} g \delta(\mu - \mu_0) \delta(\phi)$$

Note that following previous formulations (References 15 and 16), diffuse radiation is not considered in Equation (2-2). For diffuse radiation, the surface reflection is less than 4 percent. Also, it will be shown that the surface reflection of direct radiation becomes important only at low elevation angles. The bidirectional reflectance distribution function of a typical surface can be illustrated by two well-known results. For reflecting surfaces obeying Lambert's law (a diffuse reflector) and geometrical optics (a specular reflector), the bidirectional reflectance distribution functions are, respectively,

$$f_r(\theta, \phi; \theta', \phi') = \frac{a}{\pi} \text{ (diffuse reflector)} \quad (2-4)$$

$$f_r(\theta, \phi; \theta', \phi') = \frac{\rho(\theta)}{\mu} \delta(\mu - \mu') \delta(\phi' - \overline{\phi + \pi}) \text{ (specular reflector)} \quad (2-5)$$

where a is the albedo of the reflecting surface, and $\rho(\theta)$ is the Fresnel reflectivity given by

$$\rho(\theta) = \frac{1}{2} \left[\left(\frac{\sqrt{\epsilon - \sin^2 \theta} - \cos \theta}{\sqrt{\epsilon - \sin^2 \theta} + \cos \theta} \right)^2 + \left(\frac{\epsilon \cos \theta - \sqrt{\epsilon - \sin^2 \theta}}{\epsilon \cos \theta + \sqrt{\epsilon - \sin^2 \theta}} \right)^2 \right] \quad (2-6)$$

where ϵ is the dielectric constant for the reflecting element. The surface of snow has been modeled as a rough surface consisting of randomly oriented faceted grains (Reference 8). The roughness scale of the surface can be assumed to be large for visible and near-infrared radiation. Unevenness of the surface, such as snow on the ridges of a hill or ripples on a prairie snowpack and local ice crust, have not previously been considered. These factors are expected to influence the observations taken from large snowpack areas. The effect of surface topography on the reflected radiation can be studied through the bidirectional reflectance distribution function. To use the rough surface scattering theory results developed for radar cross-section analysis (Reference 18), the bidirectional reflectance distribution function defined in Equation (2-2) is related to the differential cross-section per unit area, $Y(\theta, \phi; \theta', \phi')$, generally obtained in radar analysis as:

$$f_r(\theta, \phi; \theta', \phi') = \frac{1}{4\pi \cos \theta' \cos \theta} Y(\theta, \phi; \theta', \phi') \quad (2-6)$$

$$= \frac{1}{\cos \theta \cos \theta'} \cdot \frac{R^2 |E_s|^2}{S |E_0|^2} \quad (2-7)$$

where

E_s = scattered amplitude at distance R from scattering center

S = surface area of scattering

E_0 = amplitude of incident radiation.

If there is no preferential orientation of the facets and their distribution is Gaussian (forming the so-called Gaussian isotropic surface), then from Reference 19 the bidirectional reflectance distribution function is obtained as:

$$f_r(\theta, \phi; \theta', \phi') = \frac{\sec^4 \alpha \exp \left[-\frac{\tan^2 \alpha}{2s^2} \right] S(\theta, \theta') \rho(\psi)}{8\pi s^2 \cos \theta \cos \theta'} \quad (2-8)$$

where

s^2 = variance of surface slope

$$\tan \alpha = \frac{[\sin^2 \theta + \sin^2 \theta' - 2 \sin \theta \sin \theta' \cos \phi']^{1/2}}{(\cos \theta + \cos \theta')}$$

$$\cos \psi = \frac{1}{\sqrt{2}} (1 + \cos \theta \cos \theta' - \sin \theta \sin \theta' \cos \phi')^{1/2}$$

$\rho(\psi)$ = Fresnel's Reflectivity for angle ψ .

$$S(\theta, \theta') = \frac{1}{C_0 + C_1 + 1}$$

$$2c_0 = \left(\frac{2s^2}{\pi} \right)^{1/2} \tan \theta e^{-\cot^2 \theta / 2s^2} - \operatorname{erfc} \left(\frac{\cot \theta}{s\sqrt{2}} \right)$$

$$2c_1 = \left(\frac{2s^2}{\pi} \right)^{1/2} \tan \theta' e^{-\cot^2 \theta' / 2s^2} - \operatorname{erfc} \left(\frac{\cot \theta'}{s\sqrt{2}} \right)$$

erfc = complementary error function

This reflectance distribution function resembles one previously used for snow surfaces (Reference 8).

The surface parameter s^2 may not be considered an adjustable parameter. Experimental determination of this parameter is discussed in Reference 20. From Equation (2-2) and (2-3) the intensity and flux of direct solar radiation reflected by the surface ice grains can be written as:

$$I_r(\theta', \phi') = F_0 g f_r(\theta_0, \theta; \theta', \phi') \quad (2-9)$$

$$F_r(\theta_0) = F_0 g f(\theta_0) \quad (2-10)$$

where the directional surface reflectance $f(\theta_0)$ is defined as:

$$f(\theta_0) = \int_0^{2\pi} d\phi' \int_0^1 d\mu' \mu' f_r(\theta_0, \theta; \theta', \phi'). \quad (2-11)$$

This surface reflection is primarily responsible for angular variation of radiation reflected by the snowpack.

(2) Volume Scattering Effect

Incident solar radiation not reflected by the surface will penetrate through the snowpack, getting weaker due to scattering and absorption by the ice grains. As a result of multiple scattering, a fraction of the incident flux will be reflected back into the atmosphere. The total incident flux for which the multiple scattering effect will be studied is given by (from Equations (2-1) and (2-10))

$$\begin{aligned} F &= F_0 g [1 - f(\theta_0)] + (1 - g) F_0 \\ &= F_0 [1 - g f(\theta_0)] \end{aligned} \quad (2-12)$$

This effect may be examined by studying the solution of the radiative transfer equation (Reference 21). This is the energy conservation relation for radiation propagating through a scattering and absorbing medium. The spectral absorption coefficient of ice, the grain size, shape, density and thickness of the snowpack enter into this equation through parameters called the single scattering

albedo ω , the extinction coefficient γ , the optical thickness τ , and the phase function p . The intensity of scattered radiation within the snowpack may be obtained from the solution of the following equation:

$$\mu \frac{dI(\tau, \mu)}{d\tau} = -I(\tau, \mu) + \frac{\omega(\tau)}{2} \int_{-1}^1 p(\mu, \mu') I(\tau, \mu') d\mu' + \frac{\omega F}{4\pi\mu_0} p(\mu, \mu_0) e^{-\tau/\mu_0} \quad (2-13)$$

where

I = intensity of radiation

τ = optical thickness = $\int_0^x \gamma(x') dx'$

x = depth within snow from the surface.

The single scattering albedo (ω) is defined as the ratio of scattering and extinction cross-sections of the ice grains. For this model the Mie scattering theory will be used to calculate the single scattering albedo (Reference 23). A simple formula which reproduces the Mie theory results for large spheres with reasonable accuracy (References 22 and 23) is

$$\omega = \frac{1}{2} + \frac{1}{2} \exp(-ckr)$$

where

$c = 1.67$

k = spectral absorption coefficient of ice (References 23 and 24)

r = radius of ice grains.

Although the Mie scattering calculation is based on spherical particles, it has been suggested that Equation (2-14) may be used for nonspherical particles by choosing a different value for the constant c (Reference 22) or by using the radius value of a circular area equivalent to the shadow area of the particles (Reference 25).

The extinction coefficient (γ) is the product of the extinction cross-section (σ_0) and the number density (N) of ice grains. For large spherical particles one obtains:

$$\sigma_e = 2\pi r^2 \quad (2-15)$$

$$N = \frac{3}{4\pi r^3} \left(\frac{\rho_s}{\rho_i} \right) \quad (2-16)$$

where r is the radius, and ρ_s and ρ_i are respectively the densities of snow and ice. Thus the extinction coefficient is given by

$$\gamma = \frac{3}{2r} \left(\frac{\rho_s}{\rho_i} \right) \quad (2-17)$$

The scattering phase function, $p(\mu, \mu')$, which is the ratio of differential and total scattering cross-sections can also be obtained from the Mie scattering theory. Since large particles scatter strongly in the forward direction, the phase function is strongly asymmetric (Reference 15). Further details about this function will be discussed later.

The boundary conditions for the solution of this equation are:

At the snow-air interface

$$I_+(\tau = 0, \mu) = 0 \quad (2-18)$$

and at the bottom interface, assuming soil can be treated as a Lambertian reflector, the boundary condition is

$$I_-(\tau = \tau_0, \mu) = a_s I_+(\tau = \tau_0, \mu) + \frac{a_s F}{\pi} \exp(-\tau_0/\mu_0) \quad (2-19)$$

where

a_s = albedo of soil surface

τ_0 = optical thickness of the snowpack

and, I_+ and I_- are respectively the intensities going away and towards the surface.

Accurate solution of the radiative transfer equation for strongly asymmetric phase functions is numerically difficult and time consuming. However, this asymmetric nature of the phase function has been used to develop approximations which are reasonably accurate (References 26 and 27). The

idea is to approximate the forward scattering peak by a delta function. Once the forward scattering peak is subtracted from the phase function, the remaining scattering function is amenable to efficient and accurate solutions. By writing the phase function as

$$p(\mu, \mu') = 2d^2 \delta(\mu - \mu') + (1 - d^2)p^*(\mu, \mu') \quad (2-20)$$

(where d^2 is the fraction of radiation scattered in the forward direction, and $p^*(\mu, \mu')$ is the peak subtracted normalized scattering function) one can show that the form of the radiative transfer equation remains invariant. The transformed radiative transfer equation contains, in place of parameters τ , ω , and $p(\mu, \mu')$, the new parameters τ^* , ω^* , and $p^*(\mu, \mu')$, where

$$\tau^* = (1 - \omega d^2)\tau \quad (2-21)$$

$$\omega^* = \frac{(1 - d^2)\omega}{(1 - d^2\omega)} \quad (2-22)$$

The value of d^2 for large semitransparent ice spheres is approximately 0.76 in the visible region, and 0.92 in the near-infrared region. From above discussion, these new parameters are to be used in Equations (2-13), (2-18) and (2-19) to study the volumetric scattering effect.

(3) Spectral Reflectance and Albedo

If the spectral reflectance, A_λ , is defined as the ratio of reflected and incident fluxes of monochromatic radiation, then one obtains

$$A_\lambda(\theta_0) = \frac{F_0 g f(\theta_0) + 2\pi \int_0^1 I_-(0, \mu) \mu d\mu}{F_0} \quad (2-23)$$

$$= F(\theta_0)g + [1 - g f(\theta_0)] R_d \quad (2-24)$$

where $I_-(0, \mu)$ is the intensity of volumetrically scattered emerging radiation, and

$$R_d = \frac{2\pi \int_0^1 I_-(0, \mu) \mu d\mu}{F_0 [1 - g f(\theta_0)]} \quad (2-25)$$

is the diffuse reflectance of snow. The first term on the right-hand side of Equation (2-24) is due to

surface reflection, and the second term is due to multiple scattering. Changes in surface texture and topography will affect the spectral reflectance for clear sky conditions. Since the ratio of direct and total radiation (g) depends upon the wavelength, the effect of surface texture and topography is not expected to be same for all wavelengths. From the spectral reflectance, the albedo can be calculated as:

$$A(\theta_o) = \frac{\int_0^{\infty} A_{\lambda}(\theta_o) F_o d\lambda}{\int_0^{\infty} F_o d\lambda} \quad (2-26)$$

III. Illustrative Numerical Results

The directional surface reflectances calculated for the bidirectional reflectance distribution function equation (2-8) are given in Table 1 for the surface parameter $s^2 = 0.01$. The calculation was performed using 1° azimuth grid with the Simpson's rule, and the 64 point Gauss quadrature for the elevation angle.

Table 1: Directional Surface Reflectance

| Solar Elevation (Degrees) | 5.0 | 10.0 | 15.0 | 20.0 | 25.0 | 30.0 | 35.0 | 40.0 |
|---------------------------|--------|--------|--------|--------|--------|--------|--------|--------|
| Surface Reflectance | 0.3403 | 0.2422 | 0.1739 | 0.1273 | 0.0873 | 0.0622 | 0.0458 | 0.0355 |

From the solution of the radiative transfer equation, the subsurface reflectance for a homogeneous snowpack was calculated using the following equation (Reference 28, chapter 8, and Reference 27):

$$R_d = \frac{\omega^* 2 - 3q\mu_o + (1 - \omega^*) 3a^*\mu_o(2\mu_o - q)}{2(1 + q)(1 - \delta^2\mu_o^2)} \quad (3-1)$$

where

$$a^* = d/(1 + d)$$

$$\delta = [3(1 - \omega^*)(1 - \omega^*a^*)]^{1/2}$$

$$q = 2\delta / [3(1 - \omega^* a^*)]$$

In order to calculate the spectral reflectance of snow, it is necessary to obtain the incident flux of the solar radiation. For clear sky conditions, the solar radiation incident on a snowpack can be decomposed into two parts: the direct radiation and atmospherically scattered radiation. The direct radiation incident on the surface differs significantly from the radiation incident on top of the atmosphere. Atmospheric constituents such as ozone, oxygen, carbon dioxide, and water vapor are spectrally selective absorbers of solar radiation. The relative magnitude and angular variation of atmospherically scattered radiation varies with solar elevation, atmospheric conditions and the surface reflectivity.

The spectral flux outside the atmosphere ($F_{O\lambda}$) is multiplied by parameterized attenuation coefficients of ozone (τ_{O_3}), water vapor (τ_{H_2O}), mixed gases (τ_g), aerosol (τ_a), and the Rayleigh scattering (τ_R) given in Reference 29 to obtain the direct incident flux on snow as

$$F_{\lambda}^{(1)} = F_{O\lambda} \tau_{O_3} \tau_{H_2O} \tau_g \tau_a \tau_R \sin \alpha \quad (3-2)$$

where α is the solar elevation angle. The incident atmospherically scattered radiation is calculated assuming snow albedo to be about 0.75 by the method suggested in Reference 30 from the equation

$$F_{\lambda}^{(2)} = \xi \left[F_{O\lambda} \tau_{O_3} \tau_{H_2O} \tau_g - \frac{F_{\lambda}^{(1)}}{\sin \alpha} \right] \sin^{4/3} \alpha \quad (3-3)$$

where

$$\begin{aligned} \xi &= 0.63 \text{ for } \alpha \leq 7.5^\circ \\ &= 0.602 + 0.0037\alpha \text{ for } \alpha > 7.5^\circ \end{aligned}$$

From Equations (3-2) and (3-3) one can calculate the total flux F_O , and the ratio of the direct and total fluxes g as:

$$F_O = F_{\lambda}^{(1)} + F_{\lambda}^{(2)}$$

$$g = F_{\lambda}^{(1)} / F_O$$

An equidistance grid of 45 points from 0.30 to 2.50 micron radiation is chosen to represent the incident flux. Using this representation, the spectrally integrated values are obtained by the Simpson rule method. The atmospheric parameters for a dry clear winter condition (References 29 and 30) are chosen as follows:

Ozone Path Length = 0.28 cm NTP

Water Vapor Path Length = 0.9 cm

Angstrom Aerosol coefficient = 0.08.

The calculated spectral incident flux for two different solar elevations are shown in Figure 1. Absorption of ultraviolet radiation by ozone, and near-infrared radiation by water vapor and carbon dioxide is evident in the incident solar flux. At low elevations, the redness of sky can be seen through the broadening of incident visible flux due to atmospheric scattering.

The spectral reflectance of snow calculated from Equation (2-24) is shown in Figures 2 and 3. The chosen radii (r) are typical snow crystal sizes for different stages of equi-temperature metamorphism. The overall shape of the reflectance curve does not seem to change with the crystal size or the solar elevation, but relative magnitude of various parts of the curve does vary. The spectral reflectance in the near-infrared regions shows maximum sensitivity to the crystal size and the solar elevation. A decrease in the solar elevation or the crystal size appears to have a similar effect on the spectral reflectance. Calculated reflectance is in qualitative agreement with the observation (Reference 31). The spectrally integrated directional reflectance (the albedo) obtained from Equation (2-26) is shown in Figure 4. Quantitative agreement between theory and averaged antarctic observations by Liljequist (see Reference 32) is good, but should be considered tentative because a direct comparison with the incident solar flux and the spectral reflectance cannot be made. Furthermore, corresponding to these observations the snow parameters are not exactly known and the chosen values of the atmospheric parameters may not be representative of subpolar regions. Note, however, for clear sky conditions the albedo values are more sensitive to snow parameters than the atmospheric parameters.

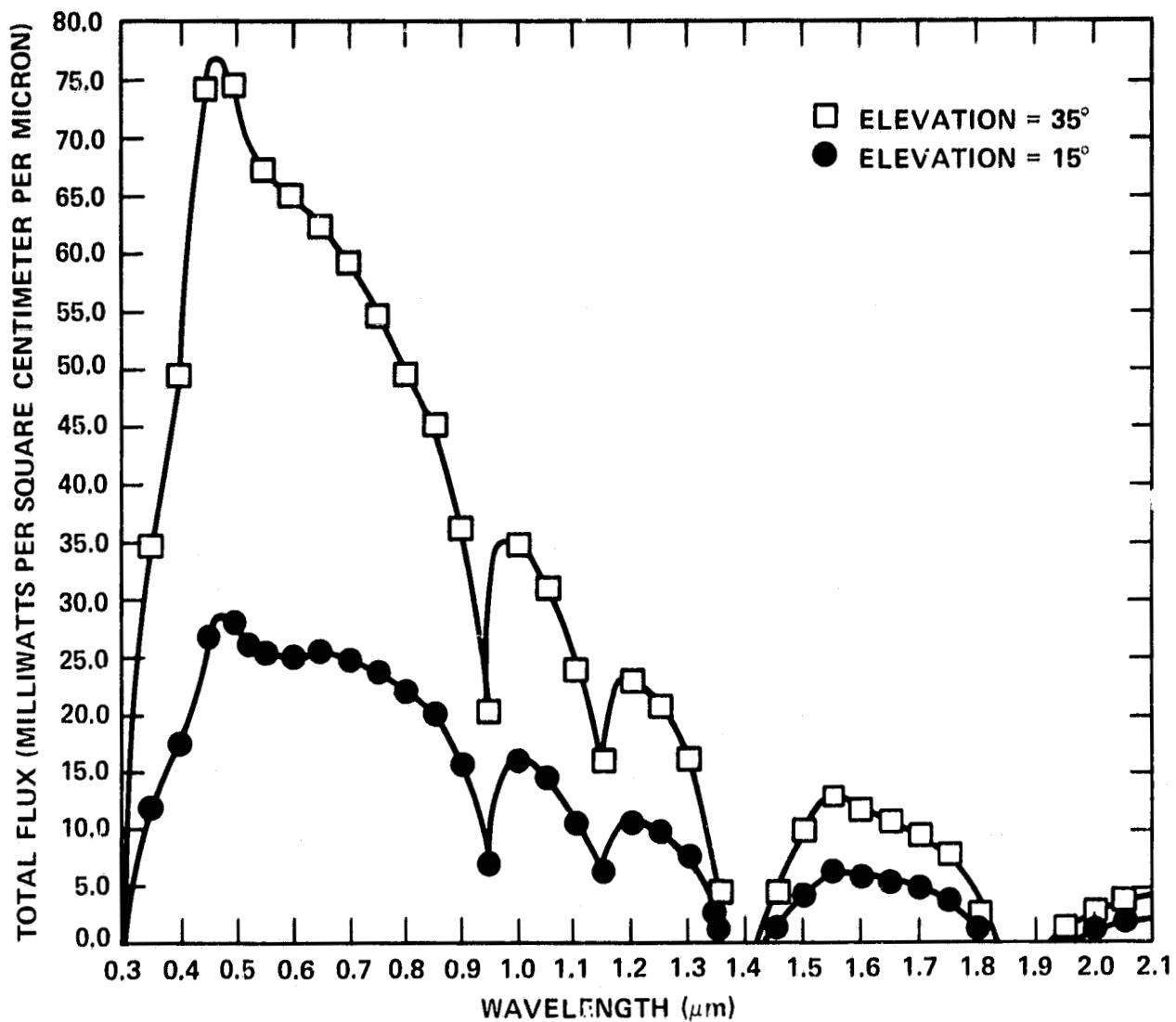


Figure 1. Spectral Variation of Incident Solar Flux

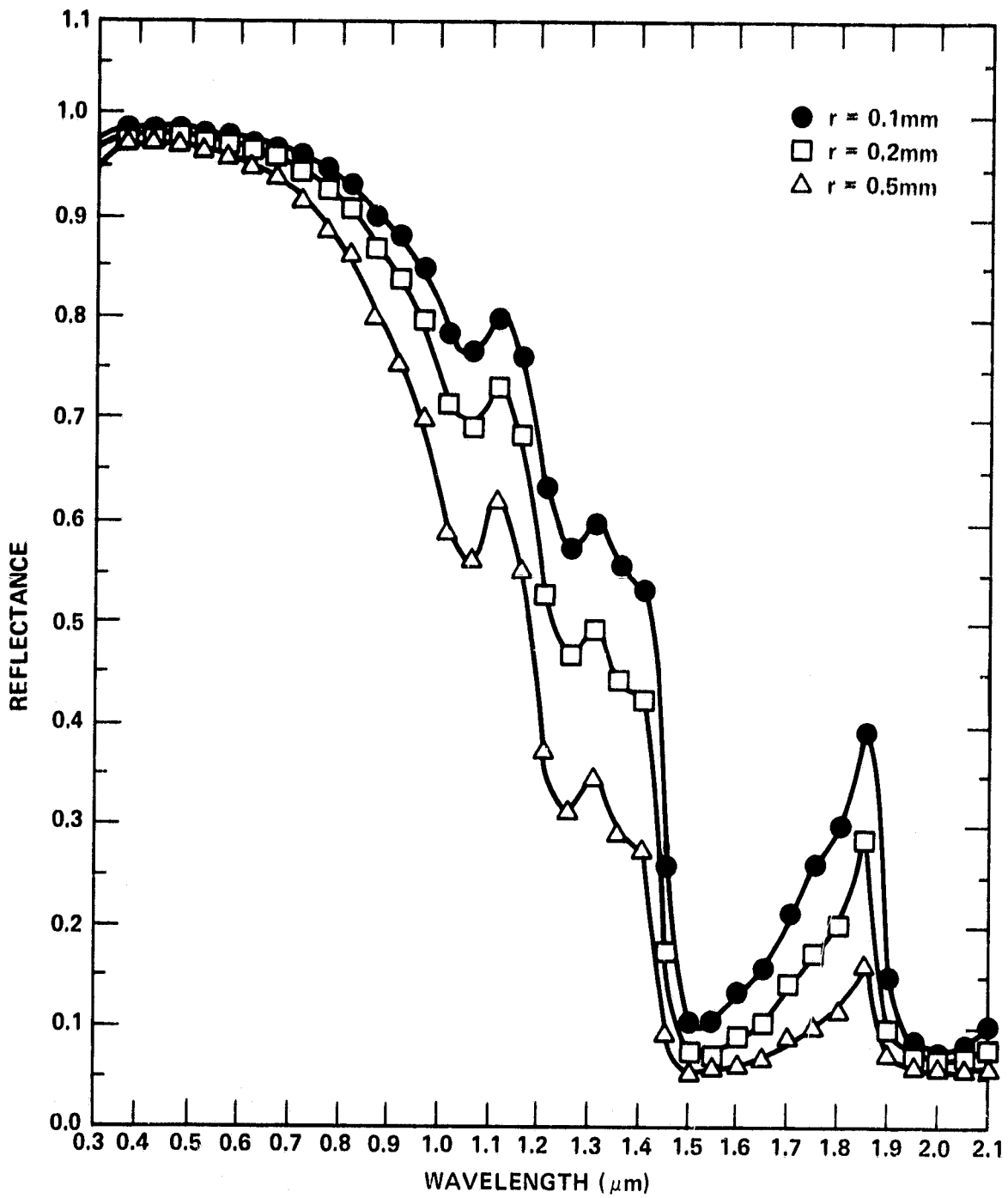


Figure 2. Spectral Reflectance of Snow for Different Grain Size for Solar Elevation of 30°

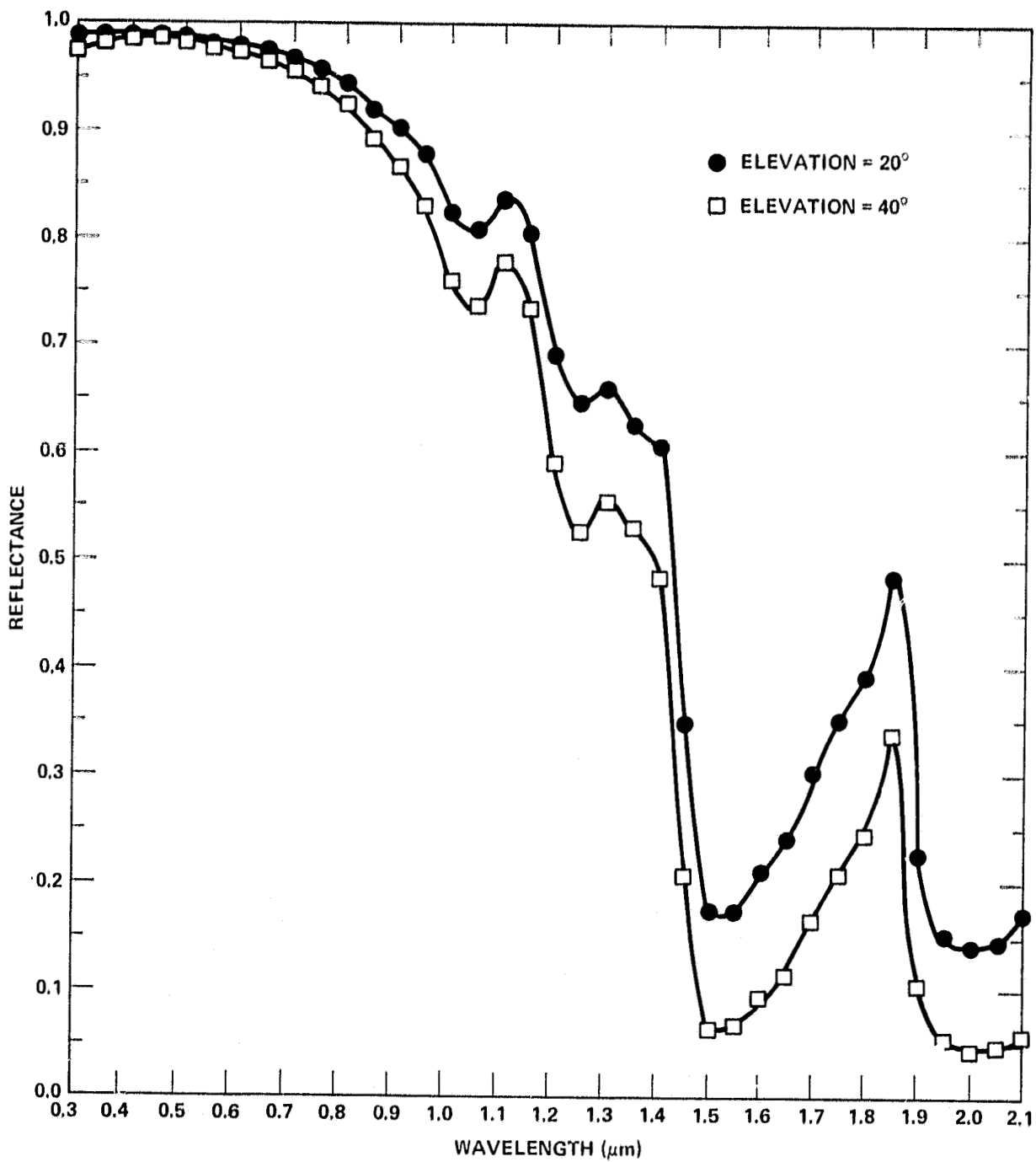


Figure 3. Spectral Reflectance of Snow for Different Solar Elevation (Grain Radius = 0.1 mm)

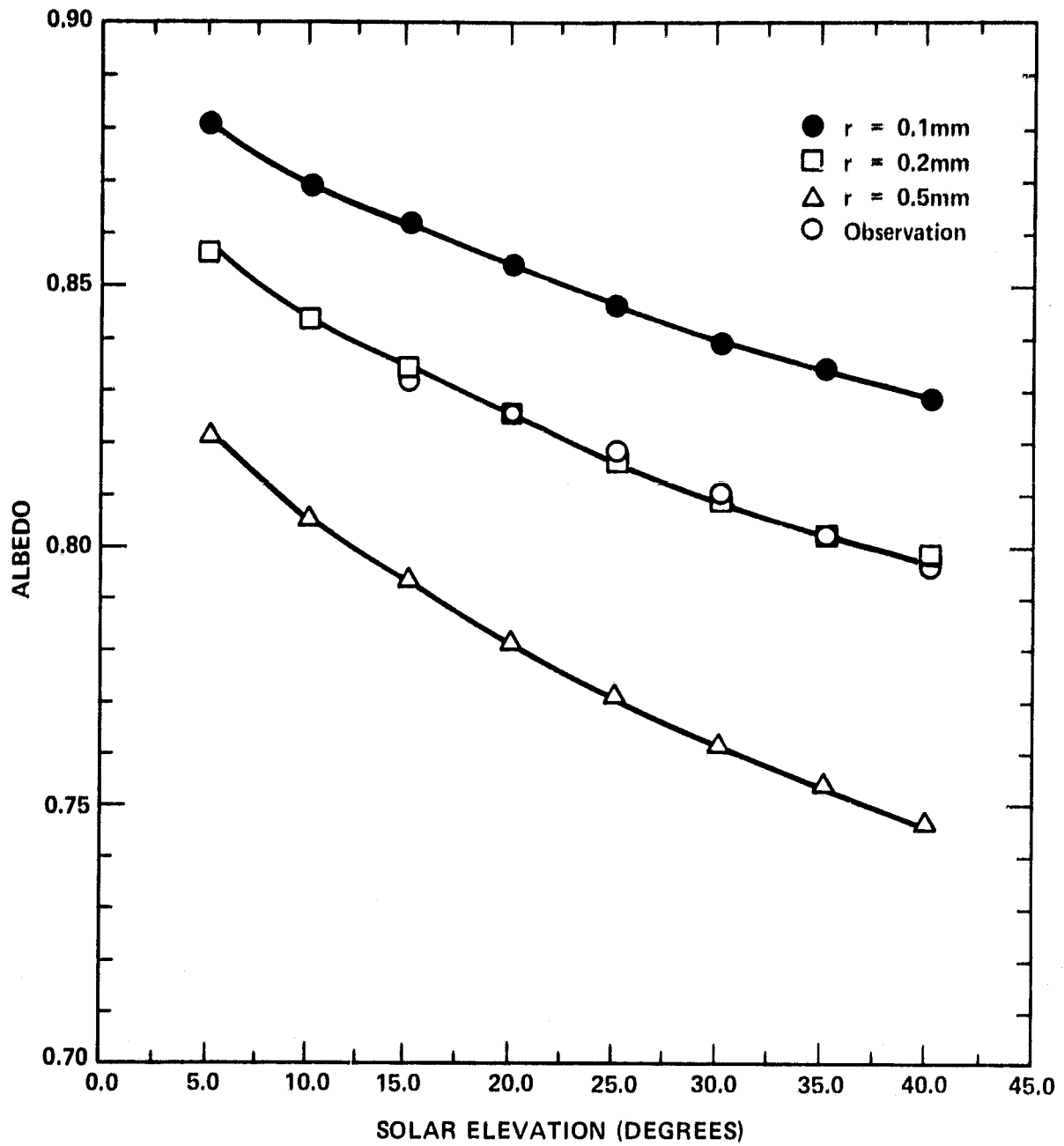


Figure 4. Dependence of Snowcover Albedo On Solar Elevation

In this study 'microscopic' surface texture (shape and orientation of surface crystals) is modeled through the parameter s in Equation (2-8). For faceted grains with more or less horizontal surfaces the value of this parameter is smaller than that for randomly oriented grains. As the value of S decreases, the magnitude of surface reflectance increases i.e., the specular surface reflection increases. The slope of the albedo - elevation curve at low elevation angles (for elevation angles less than about 25 degrees) depends primarily upon the specular surface reflection and the grain size. The slope will increase with the grain size, and higher specular reflection. At high elevation angles, the importance of surface reflection is much less than the volumetric reflection. Consequently, for these elevations, the albedo depends mainly on the grain size. The slope at low elevation angles for an old metamorphosed snow with surface crust is expected to be higher than that for a wind blown snow with rounded grains. Thus observed differences in the elevation dependence of the albedo (References 9, 12, 13, and 33) may have been due to differences in the surface texture and the grain size. A quantitative comparison with these observations would be argumentative because pertinent snow parameters are not known, and a comparison with the spectral reflectances cannot be made. A more complete set of observations is desirable.

IV. Conclusion

A model for solar reflectance of a snowpack is formulated based upon surface reflection and multiple scattering by the ice grains. The model calculations show that the surface scattering plays an important part in the angular variation of reflectance particularly for low solar elevation angles. At high solar elevation, the albedo primarily depends upon the grain size. Model calculations are in qualitative agreement with the observed spectral and integrated reflectances. Further study of this problem should be directed towards a more exact solution of the radiative transfer equation in order to study the angular dependence of multiple scattered radiation. For a better understanding of the reflective process, a more complete set of observations is needed.

References

1. S. C. Colbeck, E. A. Anderson, V. C. Bissell, A. G. Crook, D. H. Male, C. W. Slaughter, and D. R. Wiesnet, "Snow Accumulation, Distribution, Melt, and Runoff," *Transactions of American Geophysical Union*, pp. 465-468, 1979.
2. G. J. Kukla, J. K. Angell, J. Korshover, H. Dronia, M. Hoshiai, J. Namias, M. Rodewald, R. Yamamoto, and T. Iwashima, "New Data On Climatic Trends," *Nature*, 1977, vol. 270, pp. 573-580.
3. B. Choudhury and G. Kukla, "Impact of CO₂ on Cooling of Snow and Water Surfaces," *Nature*, 1979, Vol. 280, pp. 668-671.
4. J. Williams, "The Influence of Snowcover on the Atmospheric Circulation and Its Role in Climatic Change: An Analysis Based on Results from the NCAR Global Circulation Model," *Journal of Applied Meteorology*, 1975, vol. 14, pp. 137-152.
5. I. Held and M. Suarez, "Simple Albedo Feedback Models of the Icecaps," *Tellus*, 1974, vol. 26, pp. 613-629.
6. M. R. de Quervain, "On The Metamorphism of Snow," Chapter 29, *Ice and Snow*, W. D. Kingery (editor), M.I.T. Press, Cambridge, Massachusetts, 1963.
7. U.S. Department of Agriculture, Forest Service Research Paper RM-48-1969- "Classification Outline for Snow On the Ground," R. A. Sommerfeld, 1976.
8. W. E. Knowles Middleton and A. G. Mungall, "The Luminous Directional Reflectance of Snow," *Journal of The Optical Society of America*, 1952, vol. 42, pp. 572-579.
9. I. Dirmhirn and F. D. Eaton, "Some Characteristics of the Albedo of Snow," *Journal of Applied Meteorology*, 1975, vol. 14, pp. 375-379.
10. M. Mellor, "Engineering Properties of Snow," *Journal of Glaciology*, 1977, vol. 19, pp. 15-66.
11. T. C. Grenfell and G. A. Maykut, "The Optical Properties of Ice and Snow in the Arctic Basin," *Journal of Glaciology*, 1977, vol. 18, pp. 445-463.
12. V. V. Salomonson and W. E. Marlatt, "Anisotropic Solar Reflectance Over White Sand, Snow and Stratus Clouds," *Journal of Applied Meteorology*, 1968, vol. 7, pp. 475-483.

13. H. C. Korff and T. H. Vonder Haar, "The Albedo of Snow in Relation to the Sun Position," pp. 236-238, *Conference on Atmospheric Radiation*, American Meteorological Society, Fort Collins, Colorado, 1972.
14. E. S. Batten, "The Reflectance Characteristics of Snow Covered Surfaces," pp. 291-295, *Fourth National Aeronautics and Space Administration Weather and Climate Program Science Review*, NASA Conference Publication 2076, Edited by E. R. Kreins, 1979.
15. C. F. Bohren and B. R. Barkstrom, "Theory of the Optical Properties of Snow," *Journal of Geophysical Research*, 1974, vol. 76, pp. 4527-4535.
16. B. J. Chondhury and A. T. C. Chang, "Two Stream Theory of Spectral Reflectance of Snow," *IEEE Trans. (GE)*, 1979, vol. GE-17, pp. 63-68.
17. K. E. Torrance and E. M. Sparrow, "Theory for Off-Specular Reflection From Roughened Surfaces," *Journal of the Optical Society of America*, 1967, vol. 57, pp. 1105-1114.
18. D. E. Barrick, "Rough Surfaces," Chapter 9, *Radar Cross-Section Handbook*, Edited by G. T. Ruck, New York, Plenum Press, 1970.
19. M. I. Sancer, "Shadow-Corrected Electromagnetic Scattering from a Randomly Rough Surface," *IEEE Transaction On Antennas and Propagation*, 1969, vol. AP-17, pp. 577-585.
20. W. A. Rense, "Polarization Studies of Light Diffusely Reflected from Ground and Etched Glass Surfaces," *Journal of the Optical Society of America*, 1950, vol. 40, pp. 55-59.
21. S. Chandrasekhar, *Radiative Transfer*, Chapter 1, New York, Dover Publication, 1960.
22. C. Sagan and J. B. Pollack, "Anisotropic Nonconservative Scattering and the Clouds of Venus," *Journal of Geophysical Research*, 1967, vol. 72, pp. 469-477.
23. W. M. Irvine and J. B. Pollack, "Infrared Optical Properties of Water and Ice Spheres," *ICARUS*, 1968, vol. 8, pp. 324-360.
24. P. V. Hobbs, *Ice Physics*, Oxford, Clarendon Press, 1974.
25. S. Asano, M. Sato, and J. E. Hansen, "Scattering by Randomly Oriented Ellipsoids: Application to Aerosol and Cloud Problems," pp. 265-269, NASA Conference Publication 2076, 1979.

26. È. Schaller, "A Delta-Two-Stream Approximation in Radiative Flux Calculations," *Contributions to Atmospheric Physics*, 1979, vol. 52, pp. 17-26.
27. J. H. Joseph, W. J. Wiscombe and J. A. Weinman, "The Delta-Eddington Approximation for Radiative Flux Transfer," *Journal of the Atmospheric Sciences*, 1976, vol. 33, pp. 2452-2459.
28. V. V. Sobolev, *Light Scattering in Planetary Atmosphere*, New York, Pergamon Press, 1975.
29. B. Leckner, "The Spectral Distribution of Solar Radiation at the Earth's Surface—Elements of a Model," *Solar Energy*, 1978, vol. 20, pp. 143-150.
30. N. Robinson (editor) *Solar Radiation*, pp. 117-120, New York, Elsevier Publications, 1966.
31. M. Kuhn and L. Siogas, "Spectroscopic Studies at McMurdo, South Pole, and Siple Stations During the Austral Summer 1977-78," *Antarctic Journal of U.S.*, 1978, vol. 13, pp. 178-179.
32. B. R. Barkstrom, "Some Effects of Multiple Scattering on the Distribution of Solar Radiation in Snow and Ice," *Journal of Glaciology*, 1972, vol. 11, pp. 357-368.
33. N. N. Bryazgin and A. P. Koplev, "Spectral Albedo of Snow-ice Cover," *Problemy Arktiki i Antarktiki*, 1969, vol. 33, pp. 79-83.

BIBLIOGRAPHIC DATA SHEET

| | | | |
|---|--|---|------------|
| 1. Report No. FM 80576 | 2. Government Accession No. | 3. Recipient's Catalog No. | |
| 4. Title and Subtitle On the Angular Variation of Solar Reflectance of Snow | | 5. Report Date 1979 | |
| | | 6. Performing Organization Code | |
| 7. Author(s) B. J. Choudhury and A. T. C. Chang | | 8. Performing Organization Report No. | |
| 9. Performing Organization Name and Address Goddard Space Flight Center Greenbelt, Md. 20771 | | 10. Work Unit No. 913 | |
| | | 11. Contract or Grant No. | |
| | | 13. Type of Report and Period Covered | |
| 12. Sponsoring Agency Name and Address National Aeronautics and Space Administration Washington, DC 20546 | | 14. Sponsoring Agency Code | |
| | | 15. Supplementary Notes | |
| 16. Abstract Spectral and integrated solar reflectance of non-homogeneous snowpacks are derived assuming surface reflection of direct radiation and subsurface multiple scattering. For surface reflection, a bidirectional reflectance distribution function derived for an isotropic Gaussian faceted surface is considered and for subsurface multiple scattering, an approximate solution of the radiative transfer equation is studied. Solar radiation incident on the snowpack is decomposed into direct and atmospherically scattered radiation. Spectral attenuation coefficients of ozone, carbon dioxide, water vapor, aerosol and molecular scattering are included in the calculation of incident solar radiation. Illustrative numerical results are given for a case of North American winter atmospheric condition. The calculated dependence of spectrally integrated directional reflectance (or albedo) on solar elevation is in qualitative agreement with available observations. | | | |
| 17. Key Words (Selected by Author(s)) | | 18. Distribution Statement STAR Category 43 Unclassified--Unlimited | |
| 19. Security Classif. (of this report) Unclassified | 20. Security Classif. (of this page) Unclassified | 21. No. of Pages | 22. Price* |